Proceedings of ICRC 2001: 3 © Copernicus Gesellschaft 2001

ICRC 2001

The primary proton spectrum in the range $0.5 \div 50$ TeV from the observation of hadrons at EAS-TOP

A. Castellina, on behalf of the EAS-TOP Collaboration

Istituto di Cosmogeofisica del CNR and INFN, Torino, Italy

Abstract. The primary cosmic ray proton spectrum in the energy range $0.5 \div 50$ TeV is obtained from the hadron energy spectrum recorded by the EAS-TOP Hadron Calorimeter (Campo Imperatore, National Gran Sasso Laboratory, 2000 m a.s.l.). The hadron flux at $820\ g\ cm^{-2}$ has been measured in the range $30\ GeV \div 10\ TeV$, where it is well described by a single power law $S(E_h) = (2.25 \pm 0.20 \pm 0.34^{sys})\ 10^{-7} (\frac{E_h}{1000})^{(-2.79 \pm 0.06)}\ (m^2 s\ sr\ GeV)^{-1}$. The Corsika/QGSJET simulation is used to interpret the data; it is verified that the code describes well the hadron propagation by reproducing the ratio of hadron fluxes as measured at $820\ g\ cm^{-2}$ and sea level respectively by EAS-TOP and KASCADE experiments, in the considered energy range. The heavier nuclei component is subtracted in accordance to the expectations from direct measurements. The results on the primary proton spectrum are presented and the procedure of data analysis and accuracy of the measurement are discussed.

1 Introduction

The hadron spectrum is measured at the atmospheric depth of $820\ g\ cm^{-2}$ by means of the EAS-TOP calorimeter, in the energy range $30\ GeV \div 10\ TeV$.
Such spectrum, which includes surviving primaries and secondaries produced in the interactions in atmosphere, retains significant information about the primary energy/nucleon spectrum, thus dominated by the proton primary component, in a primary energy range in which the crossing of different experimental data is quite important.
The primary proton spectrum is derived from such data, in the energy range $0.5 \div 50\ TeV$, by means of: a) a simulation of the cosmic ray propagation in the atmosphere based on the CORSIKA code with QGSJET interaction model (Capdevielle J.N. et al., 1992; Kalmykov N.N. et al., 1993); b) the subtraction of the Helium contribution to the total flux (with maximum uncertainty $\simeq 15\%$), calculated by using its flux as derived from the direct measurements and the quoted interaction model.
The CORSIKA/QGSJET code is checked with good consistency by comparing the calculated and measured hadron fluxes at the EAS-TOP and KASCADE atmospheric depths (820 and $1000\ g\ cm^{-2}$ respectively).
The hadron flux measurement, the verification of the interaction model used for the interpretation of the data and the derived proton flux are presented and discussed, with their systematic uncertainties.

Correspondence to: A.Castellina (castellina@to.infn.it)

2 The detector

The EAS-TOP Extensive Air Shower array (Aglietta et al., 1993) is located at Campo Imperatore, $2005\ m$ a.s.l., above the underground Gran Sasso Laboratories. The EAS-TOP Muon and Hadron Detector (Adinolfi R. et al., 1999) is a $140\ m^2$ calorimeter made of nine planes, each composed by a $13\ cm$ Fe absorber (except for the uppermost plane which is unshielded), two layers of streamer tubes and one layer operating in "quasi-proportional" mode, for a total depth of $818.5\ g\ cm^{-2}$. The tubes are $12\ m$ long, with $(3 \times 3)\ cm^2$ section and operate with a $(50\% + 50\%)$ Argon and Isobutane mixture. The streamer tubes act as tracking detectors; the "quasi-proportional" ones are used to record high particle densities, i.e. for hadron calorimetry, and operate in saturated proportional mode. The signal charge is picked up by an external matrix of $840\ (40 \times 38)\ cm^2$ pads placed on top of the tubes; the pad signals are transferred to charge integrating ADCs with 15 bit dynamical range, saturation occurring at 1 nC ($\simeq 1200$ particles).
A set of $(80 \times 80)\ cm^2$ scintillators is lodged below two absorber layers; each of them is centered on a pad and discriminated at the level of 30 particles, corresponding to an energy threshold of about $30\ GeV$; three of them are used for the present analysis. Their logical OR, which generates the read out of the whole detectors, defines the "local hadron trigger", its frequency being $f_h \simeq 0.06\ Hz$.

3 Trigger and calibration

An event is further accepted as a hadron, in the angular acceptance window, if : a) the track crosses at least three consecutive planes of the calorimeter, including the one positioned immediately below the trigger scintillators and excluding the uppermost unshielded one; b) the maximum energy is recorded on the pad belonging to the "tower" formed by the pads below the triggering scintillator on all the three planes.
The full trigger efficiency, including the above defined and the scintillator one, is greater than 65% above about $130\ GeV$ for vertical incidence; it goes down to 10% of this value for $\theta = 30^{\circ}$.
The total charge induced on the 8 inner planes, each over the area of (3×3) pads corresponding to the scintillator position is measured and then converted to the equivalent number of vertical particles by means of periodical calibration runs using a single muon trigger (pressure and temperature dependence of the induced charge being corrected for) (Adinolfi R. et al., 1999).
The energy calibration has been obtained by simulating the detector response by means of a Monte Carlo based on the GEANT code (GEANT Group , 1994). Particular care has been put in the modelling of the chamber behaviour in quasi proportional mode; the saturation in the collected charge has been studied in detail and included in the simulation, as fully discussed in (Adinolfi R. et al., 1999).
The simulation code has been experimentally checked by comparing the response to simulated electromagnetic showers to the ones obtained during a run test at CERN with a positron beam, up to a maximum particle density on the chamber corresponding to hadron energy $E_h \simeq 650\ GeV$ in the experimental conditions.
Protons at fixed primary energy and zenith angle have been generated and analysed with the same procedure as the experimental data. The conversion curve from the total number of particles induced in the calorimeter to the primary hadron energy is shown in Fig.1. The energy resolution amounts to $\simeq\ 15\%$ at $1\ TeV$, worsening to $\simeq\ 25\%$ at $5\ TeV$ due to leakage losses and to 30% at $30\ GeV$ due to sampling losses. Above the TeV region, where no direct calibration is available, the goodness of the model has been checked by comparing the simulated and experimentally measured transition curves of hadronic showers. The mean longitudinal profile of real and simulated events are in good agreement up to 5 TeV, the differences near the maximum of the shower development being within 10%.

4 The hadron flux

From a total of about 10^6 triggers, 40832 (summed over all the used "towers") survived the reconstruction and selection criteria and were classified as hadrons, either single or in showers, in a total observation time of $615\ days$. The effective collection area $A(E_h, \theta)$ has been calculated using the

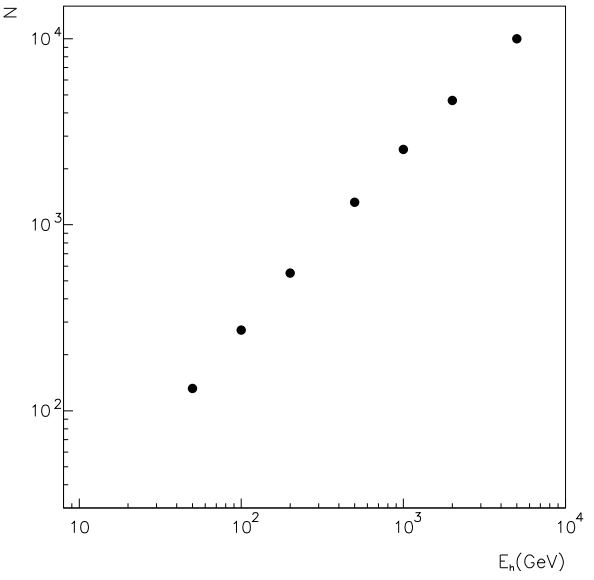

Fig. 1. Total number of induced equivalent particles versus hadron energy.

GEANT code. Each event is given an energy on the basis of the particle-energy conversion curve of Fig.1. The measured number of events in each energy bin is

$$n_{ev}^{meas}(E_h \div E_h + \Delta E_h, x) \quad = \int_{\Omega} \int_{E_h}^{E_h + \Delta E_h} S(E_h, \theta, x) T A(E_h, \theta) d\Omega dE_h \qquad (1)$$

where $A(E_h, \theta)$ is the effective area at zenith angle θ and the hadron flux at depth x is

$$S(E_h, \theta, x) = S(E_h, x) exp(-\frac{x(\theta) - x}{\Lambda(E_h)}) \qquad (2)$$

$\Lambda(E_h)$ being the attenuation length obtained through simulations.

The experimental single hadron flux at the atmospheric depth $x = 820\ g\ cm^{-2}$ is shown in Fig.2; between $30\ GeV$ and $30\ TeV$ it is well represented by a power law

$$S(E_h) = (2.25 \pm 0.20 \pm 0.34^{sys})\ 10^{-7} \left(\frac{E_h}{1000\ GeV}\right)^{(-2.79 \pm 0.06)} m^{-2} s^{-1} sr^{-1} GeV^{-1} \qquad (3)$$

Different fits in separated and independent energy regions show that the data are compatible within the experimental uncertainties with a power law spectrum with a single slope in the whole considered energy range.
The systematic uncertainties (14% energy dependent, which are included in Fig.2 and in Expr.3, and 15% on the normalization factor) are due to uncertainties in: a) detector acceptance ($\simeq 12\%$); b) energy determination ($\simeq 7\%$); c) technical calibrations, including uniformity and stability ($\simeq 15\%$).

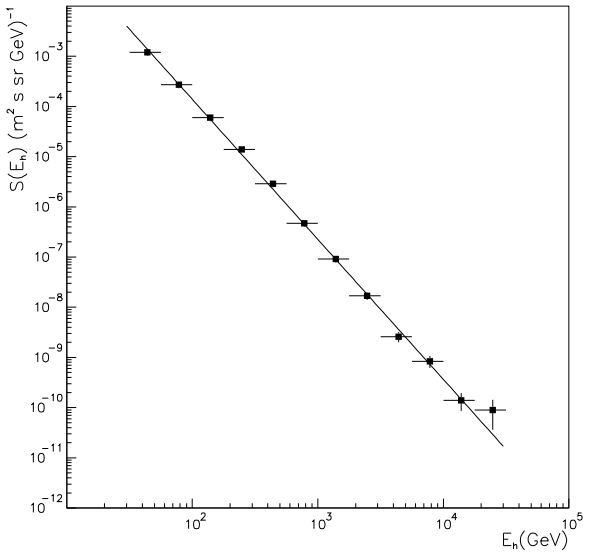

Fig. 2. *The single hadron flux at* $820\ g\ cm^{-2}$ *as measured by EAS-TOP.*

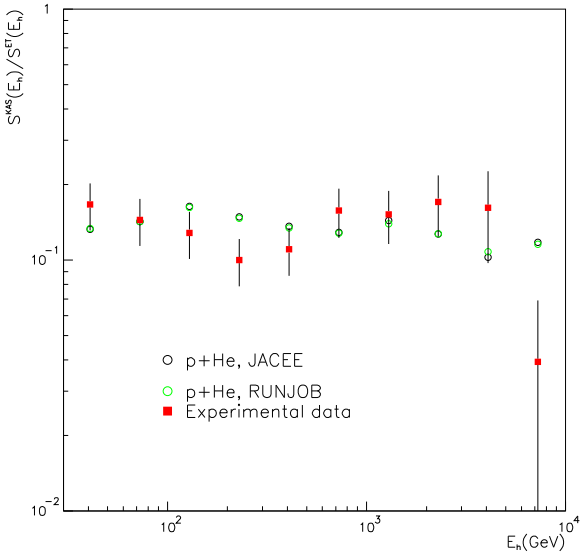

Fig. 3. *Ratio of the experimentally measured hadron fluxes by KASCADE and EAS-TOP (red squares) compared to the expectation if the proton+Helium primary spectra by JACEE (black circle) or RUNJOB (green square) are assumed.*

5 The primary proton spectrum

As a first step, the interaction model and the code used for the cosmic ray interaction and propagation in the atmosphere (CORSIKA/QGSJET) have been tested by comparing their predictions to the measured ratio of hadron fluxes at sea level (KASCADE, $1000\ g\ cm^{-2}$) and mountain altitude (EAS-TOP, $820\ g\ cm^{-2}$).
The simulation has been performed generating primary protons and Helium nuclei in quasi vertical direction ($\theta \leq 5°$), with spectral slope $\gamma = -2.75$; assuming that hadrons be produced by primary protons and Helium nuclei with spectra given by the most recent direct measurements (JACEE Coll., 1997; RUNJOB Coll., 1997), the expected number of events in each energy bin is calculated at each given observation level.
The comparison between the calculated and the measured ratios is shown in Fig.3: the experimental ratio is well reproduced by the simulation, independently on the used primary composition, in the whole available energy range $100\ GeV \div 10\ TeV$. We are thus allowed to use it in the same energy range between the top of the atmosphere and the observation level of EAS-TOP.
The primary energies contributing to the hadrons measured at EAS-TOP span the range from $500\ GeV$ to $50\ TeV$.
The contribution to the measured hadron flux from Helium primaries is evaluated using the Helium spectrum as measured by JACEE or RUNJOB; at $E_h \simeq 1\ TeV$ it amounts to $\simeq 23\%$ and $\simeq 27\%$ respectively. After subtracting it from the experimentally measured all hadron flux, the fraction of hadrons generated by primary protons is obtained.

The parameters Φ_0 and γ of the primary proton flux $d\Phi/dE = \Phi_0 E^{-\gamma}$ are obtained by means of a χ^2 procedure fitting the experimental data in all the energy bins of Fig.2.
In order to be free from any hypotheses on the slope of the primary spectrum, all the available hadron data have been divided in independent $\Delta E_h = 0.1 \div 0.2,\ 0.2 \div 0.5,\ 0.5 \div 1,\ 1 \div 2,\ 2 \div 5, \geq 5\ TeV$ energy bins, and the previously described procedure has been repeated for each of the median primary energies contributing to them. In fact, the main contribution to each hadron energy bin at the experimental depth comes from different regions of primary spectrum.
The data are compatible with a single power law describing the primary proton spectrum in the range $0.5 \div 50\ TeV$.
The resulting spectrum is shown in Fig.4 for the case of subtraction of the expected hadron contribution from Helium according to JACEE (black full squares) and according to RUNJOB (empty black squares). Results from other experiments are also shown.
An expanded view of the explored energy region is shown in Fig.5, where the proton flux has been multiplied by $E^{2.7}$.
The systematic error on the absolute flux depends mainly on the contamination of the sample by heavier nuclei; together with the error of about 18% due to the uncertainty in the measured hadron flux (which is included in the plot), this results in a total systematic uncertainty of $\simeq 25\%$ on the primary proton spectrum.

6 Conclusions

The hadron flux has been measured by means of the EAS-TOP calorimeter at $820\ g\ cm^{-2}$ in the range $30\ GeV \div$

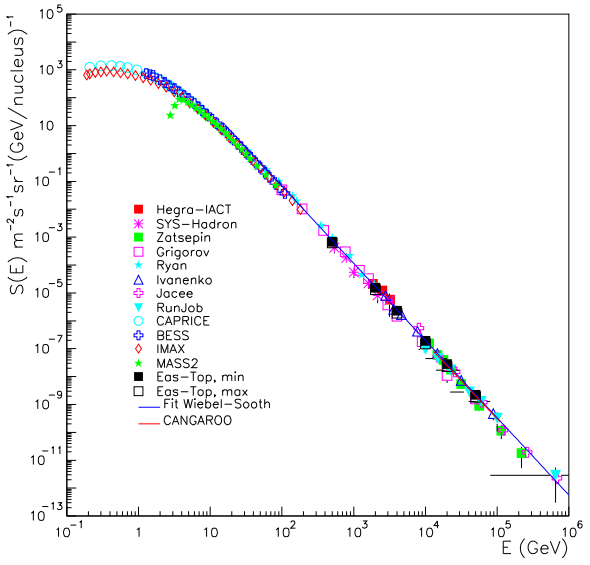

Fig. 4. *Primary proton spectrum.The black points show the present result having subtracted the minimum (full squares) and maximum (empty squares) Helium contribution. Results are shown for comparison from (Aharonian et al., 1999), (Inoue et al., 1997),(Zatsepin et al., 1993),(Swordy S., 1993),(Grigorov N.L., 1999), (JACEE Coll., 1997),(RUNJOB Coll., 1997),(Boezio et al., 1999),(Sanuki T., 1999),(Menn et al., 2000), (Bellotti et al., 1999),(Sakurazawa et al., 1997); a global fit from (Wiebel–Sooth et al., 1998) is also plotted.*

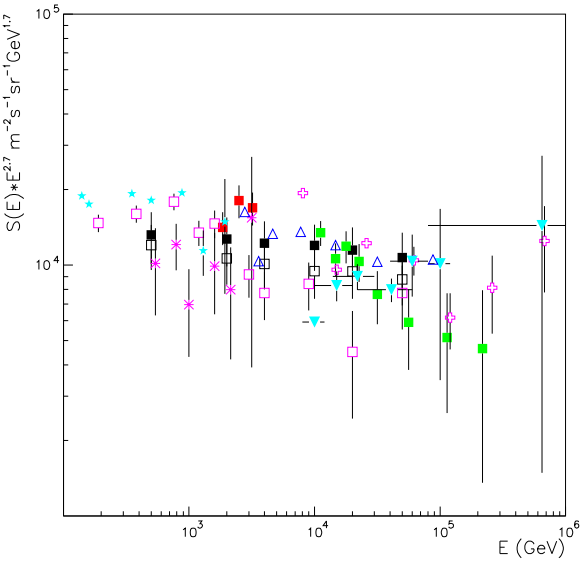

Fig. 5. *Primary proton spectrum multiplied by $E^{2.7}$ from EAS-TOP (empty and full black squares). Symbols as in the previous figure.*

$10\ TeV$; it is well described by a single power law $S(E_h) = (2.25 \pm 0.20 \pm 0.34^{sys}) \times 10^{-7} (\frac{E_h}{1000})^{(-2.79 \pm 0.06)}$ $m^{-2} s^{-1} sr^{-1} GeV^{-1}$.

From such measurement, the primary proton spectrum in the energy range $500\ GeV \div 50\ TeV$ has been derived: $S(E) = (9.6 \pm 1.9 \pm 2.4^{sys}) \times 10^{-2} E^{(-2.75 \pm 0.09)}$ $m^{-2} s^{-1} sr^{-1} GeV^{-1}$.

The contamination from heavier nuclei has been taken into account based on direct data and a model for the cosmic rays propagation and interaction in the atmosphere. The total systematic uncertainty is $\simeq 25\%$. A single power law spectrum is compatible with the data over the whole energy range. The measurement is not a direct one, but the used hadronic interaction model (CORSIKA/QGSJET) was checked by comparing with independent experimental data and a very good reliability was obtained in the whole considered energy range.

References

Adinolfi R. et al. (EAS-TOP Collaboration), *Nucl.Instr. and Meth. in Phys.Res.*, **A420** (1999) 117.

Aglietta M. et al. (EAS-TOP Collaboration), *Nucl.Instr. and Meth. in Phys.Res.*, **A336** (1993) 310.

Aharonian F. et al,*Phys.Rev.D* **59** (1999) 092003.

Bellotti R. et al., *Phys.Rev.***D60** (1999) 052002.

Boezio M. et al., *The Astrop.J.***518** (1999) 457.

J.N.Capdevielle, KfK 4998 (1992); J.Knapp et al., KfK **5196B** (1993).

Application Software Group and Network Division, *GEANT: Detector description and Simulation tool 3.21*, CERN **W5013** (1994).

Inoue N. et al., *Proc.25rd ICRC*, **4** Durban (1997) 113.

JACEE Coll., *Proc. 25th Int.Cosmic Ray Conf.*, **4** Durban (1997) 1.

Kalmykov N.N. Ostapchenko S.S., *Yad.Fiz.***56** (1993).

Menn W. et al., *The Astrop.J.***533** (2000) 281.

RUNJOB Coll., *Proc. 25th Int.Cosmic Ray Conf.*, **4** Durban (1997) 131,144.

Sakurazawa K. et al., *Proc.25rd ICRC*, **3** Durban (1997) 165.

Sanuki T. et al.,*Proc. 26th ICRC***3** Salt Lake City (1999) 93.

Swordy S., *Proc.23rd ICRC*,Rapporteur Papers, Calgary (1993) 243.

Swordy S., *Proc.26th ICRC*, **3** Salt Lake City (1999) 183.

Wiebel–Sooth B. et al.,*Astron.Astroph.* **330** (1998) 389.

Zatsepin V.I. et al,*Proc.23rd ICRC* **2** Calgary (1993) 13.